Resistance, Magnetoresistance, and Thermopower of Zinc Nanowire Composites

Joseph P. Heremans, Christopher M. Thrush, Donald T. Morelli, and Ming-Cheng Wu

Delphi Research Labs, Shelby Township, Michigan 48315, USA

(Received 1 April 2003; published 14 August 2003)

We report a very large enhancement of the thermopower of 4 nm diameter metallic Zn nanowires, with a temperature dependence that is consistent with that of their electrical resistivity and the Mott formula. The temperature dependence of the resistance, magnetoresistance, and thermopower of composites consisting of 15, 9, and 4 nm diameter Zn nanowires imbedded in porous host materials is reported. The 15 nm wires are metallic. The smaller wires show 1D weak localization, but the electrical resistivity mostly follows a $T^{-1/2}$ law, and the thermopower of the 4 nm wires saturates at $-130\ \mu$V/K.

DOI: 10.1103/PhysRevLett.91.076804 PACS numbers: 72.15.Jf, 73.63.Bd, 73.63.Hs

For metals to be good thermoelectric materials, they require [1] a room temperature Seebeck coefficient exceeding 100 to 150 μV/K. To our knowledge, this value has not been observed to date. In a recent Letter [2], we reported a very large increase of the thermoelectric power of bismuth nanocomposites, consisting of Bi nanowires with diameters of 15 nm in porous silica, and of 9 nm in porous alumina. In principle [3], this effect is ascribed to one-dimensional (1D) size quantization, which transforms the bulk Bi semimetal into a semiconductor. The peaks in the electronic density of states that are the signature of a 1D system result in an increase in thermopower. However, localization effects have also been observed in Bi [4] and Sb [5] nanowire systems and are expected to increase the electrical resistance with a much more modest accompanying enhancement of thermopower. The Zn nanowire system we study here remains metallic. The transport in 15 nm wires is conventional; the magnetoresistance of the smaller wires shows clear signs of weak localization, but the temperature dependence of the resistivity is larger than weak localization alone would warrant, and the magnitude of the Seebeck coefficient attains 130 μV/K, to our knowledge, the largest value measured on a metallic system. The temperature dependence of the resistivity follows a power law, $T^{-1/2}$, which, according to the Mott formula for the thermopower, is consistent with the experimentally observed thermopower.

The Zn nanocomposite samples were similar to the Bi nanocomposites used in previous work [2]. Three porous host materials were used here to prepare Zn nanocomposites, silica gel (pores on the order of 15 nm), porous Al_2O_3 with a pore size distribution centered around 9 nm, and commercially available porous Vycor [6] glass, with pore sizes on the order of 4 nm. The first two host materials were described previously [2]. The samples were impregnated with Zn using a vapor-phase technique described for Bi [7], but with slightly different processing temperatures Briefly, freestanding plates of the host material, about 0.5 mm thick, were put on top of a crucible in a cryopumped vacuum chamber, with a base pressure on the order of 10^{-8} Torr. The host material plates were equipped with a heater on their top face, which was heated near 640 °C for outgassing. Subsequently, the crucible heater was used to reach a temperature near 480 °C, to expose the porous host material to Zn vapor; then the crucible and the sample were slowly cooled, allowing the Zn vapor to condense inside the host material. From this point on, the Zn nanowires remain completely encapsulated by the host material.

We prepared one sample of the 15 nm Zn/SiO_2 composite, two samples of the 9 nm Zn/Al_2O_3 composite, and two samples of the 4 nm Zn/Vycor composite. The properties of these five samples and the quantities measured on them are summarized in Table I. Only the resistance and magnetoresistance were measured on the 15 nm Zn/SiO_2 composite, and on one sample of the Zn/Vycor composite. The resistance and magnetoresistance measurements were made using four leads attached to the macroscopic composite sample. Both samples of the Zn/Al_2O_3 and the second sample of the Zn/Vycor composite were used for thermopower and zero-field resistance measurements. The thermopower measurements were made by equipping the sample with a small resistive heater on one end, and heat sinking it on the other. Two absolute thermocouples were attached to the side of the sample, using Ag epoxy, to measure the temperature gradient. This technique [8] has the advantage that no electrical isolation is needed between the thermocouples and the sample, and that the copper legs of the thermocouple wires themselves can be used to probe the electrical potential. The electrical resistance measurements on the samples mounted for thermopower measurements were made using the same two wires and are therefore not four-wire measurements. There was no significant difference in the temperature dependence of the resistance of the two samples of either Zn/Al_2O_3 or Zn/Vycor. All samples were mounted in a liquid helium variable temperature cryostat, and dc measurement techniques were used. The samples' resistance was measured

TABLE I. Parameters of the five samples used in this study. d_w is the wire diameter. The third column gives the properties measured on each sample, 2 = two-contact measurement, 4 = four-contact measurement, R = resistance as a function of temperature, MR = magnetoresistance, S = thermopower as a function of temperature. The superscript $*$ denotes the quantity reported in the figures. The fourth column gives the sample resistance at 300 K, except for the last sample, where the resistance is given at 100 K. The last column gives the experimentally observed temperature dependence of the resistance.

Sample	d_w (nm)	Properties	$R(\Omega)$ $T = 300$ K	$R(T)$
Zn/SiO_2	15	4 R^*, MR^*	0.46 Ω	Metallic
Zn/Al_2O_3	9	2 R^*, MR^*, S^*	1.6 kΩ	$1500 + \frac{1900}{\sqrt{T}}$
Zn/Al_2O_3	9	2 R	87 kΩ	$2.4 \times 10^4 + \frac{1.1\times10^6}{\sqrt{T+11}}$
Zn/Vycor	4	4 R^*, MR^*	44 kΩ	$1.3 \times 10^4 + \frac{5.5\times10^5}{\sqrt{T+8}}$
Zn/Vycor	4	2 R, S^*	2.7 MΩ	$\frac{2.8\times10^7}{\sqrt{T+2}}$

using positive and negative currents, and the voltage was measured using a Keithley 617 electrometer, with a 10^{14} Ω input impedance. The thermopower was measured by applying a temperature gradient using the resistive heater, waiting for it to stabilize, and measuring the temperature and voltage gradients. The electrometer was used to measure the voltage, and the results on the Zn/Al_2O_3 sample were repeated using a Keithley 182 nanovoltmeter with an input impedance of 10^{10} Ω. The zero-field resistance of each of the five samples described here is given in Table I. The temperature dependence of the resistance, normalized to that at 300 K, is given in Fig. 1. The normalization is necessary because the filling fraction of Zn is unknown, and therefore so is the resistivity of the nanowires. The relative magnetoresistance of the three composites, normalized to the resistance at zero magnetic field at the same temperature, is given in Fig. 2. The thermopower of the 9 and 4 nm nanowire composites is given Fig. 3. For comparison, we reproduce as a full line in Fig. 3 the thermopower of bulk Zn [9]; the anisotropy of the thermopower between the values along the different axes in Zn crystals is smaller than the thickness of the line.

The resistance of the 15 nm Zn/SiO_2 composite is linear with temperature above 40 K and saturates below 10 K, with a residual resistivity ratio of 13. The magnetoresistance is also quadratic [Fig. 2(a)], following a law

$$R(H, T) = R(0, T)(1 + AH^2), \tag{1}$$

and the coefficient A is given, as a function of temperature, in the inset. This behavior is characteristic of metallic zinc.

The resistance of the 9 and 4 nm Zn wires follows essentially a $T^{-1/2}$ law. Fits to the data are shown in the last column of Table I and are shown as lines in Fig. 1.

The magnetoresistance of the narrower Zn wires show localized behavior. For 1D localization in a system with little spin-orbit scattering, we expect the correction due to weak localization effects to change the resistance R_0 at a given temperature to [10]

$$R(H, T) = R_0\left(1 + \frac{\rho_e e^2}{2\pi\hbar A}\frac{1}{\sqrt{L_\Phi^{-2} + L_H^{-2}}}\right), \tag{2}$$

where ρ_e is the impurity scattering limited value of the resistivity, A is the cross-sectional area of the wire, L_Φ is the phase-breaking length, and L_H is the magnetic length, given by

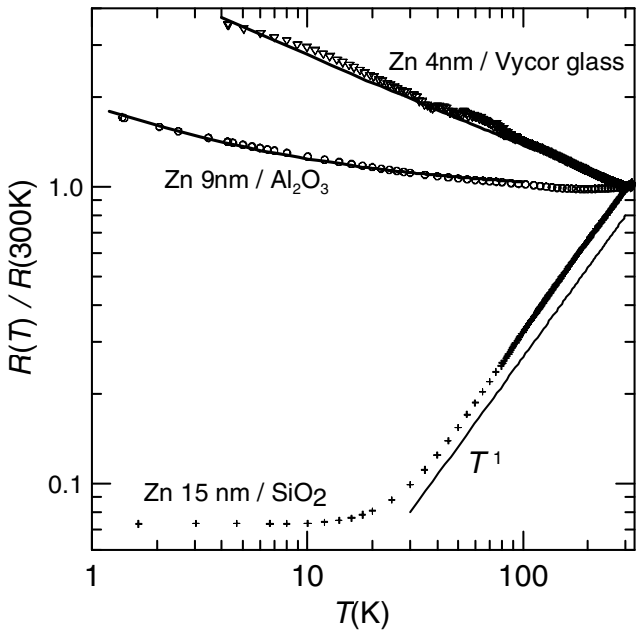

FIG. 1. Temperature dependence of the resistance of Zn nanowire composites, normalized to the resistance at 300 K. A typical metallic behavior is seen in the Zn/SiO_2 composite, with average wire diameters of 15 nm. The experimental data are shown as points; the lines are fits to $T^{-1/2}$ laws.

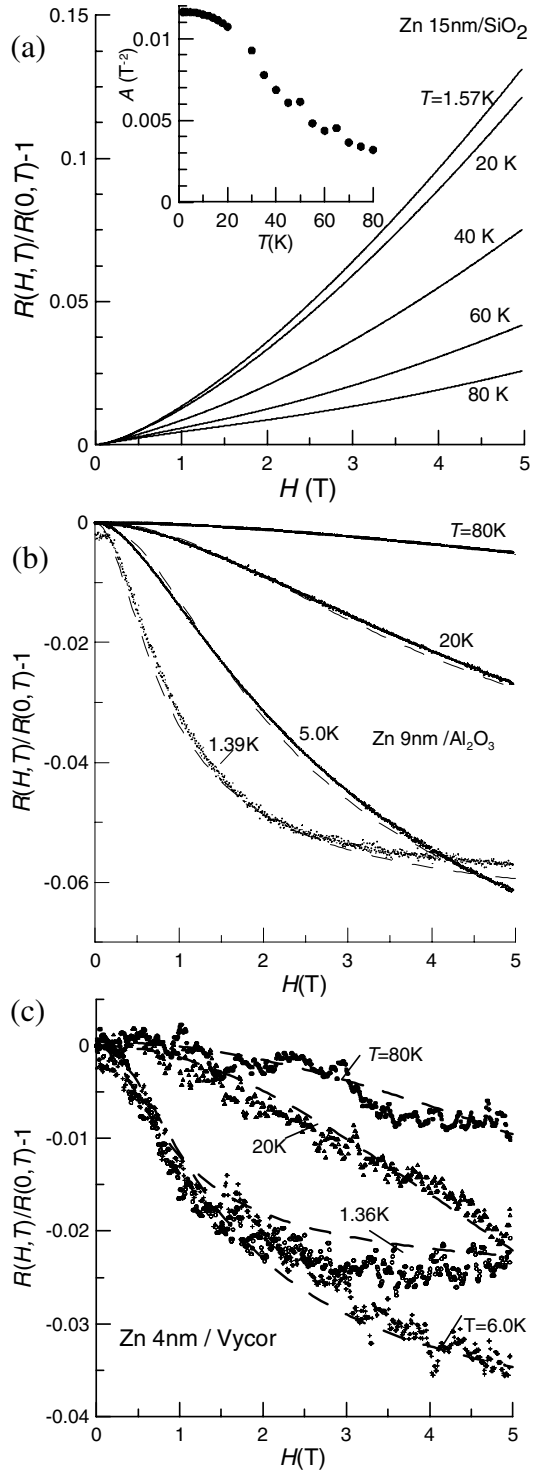

FIG. 2. Magnetic field dependence of the relative magnetoresistance of the nanocomposites studied here. The curve for each temperature is normalized to the resistance at zero field. (a) The 15 nm Zn/SiO_2 nanowires; as in bulk metals, the magnetoresistance is quadratic in field, and the coefficient A of Eq. (1) fitted to each curve is shown, as a function of temperature, in the inset. (b) For the 9 nm Zn/Al_2O_3 nanocomposite, normalized at each temperature to the resistance at zero field. (c) For the 4 nm Zn/Vycor glass nanocomposite. In frames (b) and (c), the data are given as points; the dashed lines are fits to Eq. (2).

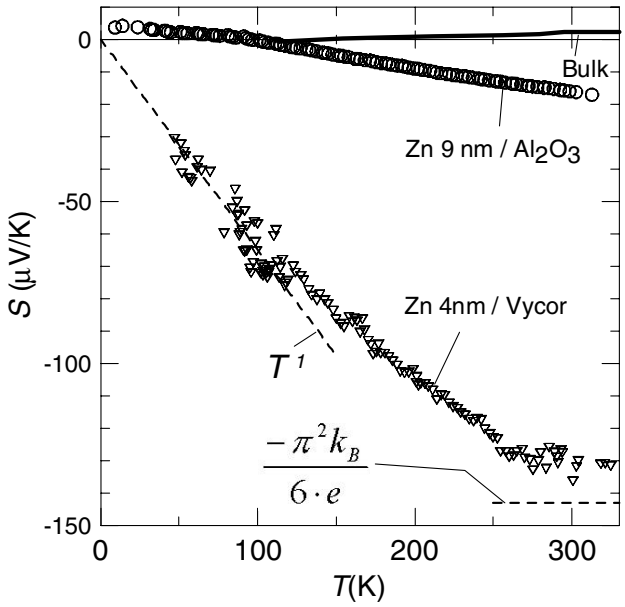

FIG. 3. Temperature dependence of the thermoelectric power of the 9 nm Zn/Al_2O_3 and of the 4 nm Zn/Vycor glass nanocomposites. Also shown is the dependence of bulk Zn, after Ref. [9].

$$L_H = \sqrt{\frac{3\hbar^2}{AH^2e^2}}. \tag{3}$$

We see in Fig. 2 that the amplitude of the magnetoresistance is at most of the order of 3% to 6%, while the zero-field resistance changes by a factor of 2 to 4, so that weak localization is a small correction to the transport, albeit one that dominates the magnetoresistance. We fit Eq. (2) to the curves Figs. 2(b) and 2(c), assuming the same value for ρ_e and treating R_0 and L_Φ as adjustable parameters. The resulting values of R_0, when plotted as a function of temperature, track the zero-field resistance very closely, as expected, since the weak localization mechanism is a small correction. The fitted values L_Φ are shown for the two samples in Fig. 4. Their absolute values are not meaningful, as they depend on the assumption made for the value of ρ_e, which we do not measure independently, but the wire diameter and the temperature dependence of L_Φ are quite as expected. While this provides evidence for the contribution of weak localization to the magnetoresistance, it also points out that weak localization does not dominate the temperature dependence of the resistance.

Turning now to the thermoelectric power results, we observe a strong deviation of the thermopower from that in bulk Zn. The thermopower of the nanowires is mostly negative, whereas that of bulk Zn is positive, and its magnitude is 1 (for the 9 nm wires) to 2 (for the 4 nm wires) orders of magnitude larger. Nevertheless, the thermopower of 9 nm Zn wires is 3 orders of magnitude smaller than that of 9 nm Bi wires, as reported in

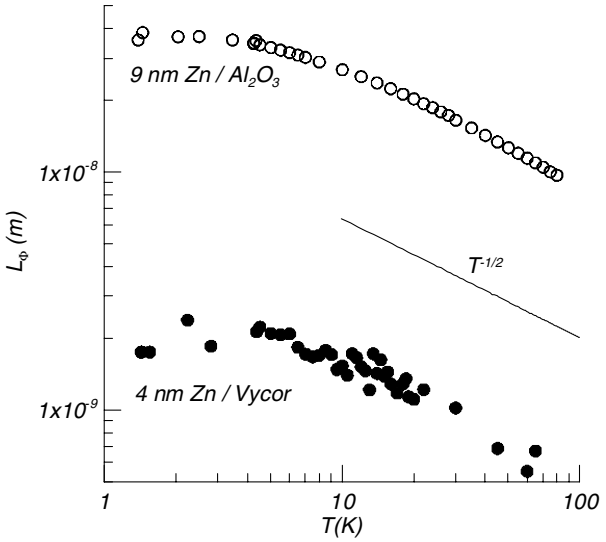

FIG. 4. Temperature dependence of the fitted phase-breaking length L_Φ of the 9 nm Zn/Al_2O_3 and of the 4 nm Zn/Vycor glass nanocomposites. The absolute value of L_Φ depends on the assumption made for the resistivity of the wires, which is not known, but its dependence on wire diameter and temperature is as shown.

Ref. [2], thus confirming that the data in that Letter cannot be ascribed to localization effects alone. According to the Mott formula, the thermopower is the logarithmic derivative of the conductivity with respect to energy:

$$S = \frac{-\pi^2 k_B^2 T}{3e} \frac{\partial \ln[\sigma(E)]}{\partial E}\bigg|_{E=E_F}. \quad (4)$$

Since we observe that the electrical conductivity's temperature dependence is given by a power law, $\sigma \propto T^{1/2}$, we can postulate that

$$\sigma(E) = a(E - E_c)^{p/2} \quad (5)$$

with $p = 1$, because the average electron energy is proportional to $k_B T$. E_c is defined as some critical energy value. In such a case, for $k_B T \ll E_c$ the thermopower is a linear function of temperature:

$$S = \frac{-\pi^2 k_B^2 T}{3eE_c} \frac{p}{2} \quad (6)$$

and for $k_B T \gg E_c$,

$$S = \frac{-\pi^2 k_B}{3e} \frac{p}{2}, \quad (7)$$

the thermopower tends to a constant. From Fig. 1, $p = 1$, and therefore the thermopower is expected to saturate near $-142\ \mu V/K$, quite close to the experimentally observed value of $-130\ \mu V/K$ in the Zn/glass system. We hesitate to ascribe a physical mechanism underlying the observed temperature dependences of σ and S and merely point out the internal consistency between the different transport results reported here.

In summary, we report experimental data on the resistivity, magnetoresistance, and thermopower of Zn nanowires in insulating matrices. Weak localization effects contribute a few percent to the overall transport, as evidenced by the magnetoresistance data below 70 K. The temperature dependence of the electrical conductivity follows a power law $T^{1/2}$, and this is consistent with the observed temperature dependence of the thermopower, which is linear up to a critical temperature, and then saturates at a value consistent with the temperature exponent of the conductivity. In 4 nm Zn wires, this value is very large for a metal, $-130\ \mu V/K$.

[1] The thermoelectric figure of merit is $Z = S^2\sigma/\kappa$, where S is the Seebeck coefficient, κ is the thermal conductivity, and σ is the electrical conductivity. If κ is dominated by electronic conduction, given by the Wiedemann-Franz law, then $ZT = S^2/L$, where L is the Lorenz number. To obtain a value of $ZT = 1$ at $T = 300$ K, one has to have a Seebeck coefficient $|S| > \sqrt{L}$, which, assuming the free electron value for L, is $157\ \mu V/K$.
[2] J. P. Heremans, C. M. Thrush, D. T. Morelli, and M. Wu, Phys. Rev. Lett. **88**, 216801 (2002).
[3] L. D. Hicks and M. S. Dresselhaus, Phys. Rev. B **47**, 16 631 (1993).
[4] J. Heremans, C. M. Thrush, Z. Zang, X. Sun, M. S. Dresselhaus, J. Y. Ying, and D. T. Morelli, Phys. Rev. B **58**, R10 091 (1998).
[5] J. Heremans, C. M. Thrush, Y.-M. Lin, S. B. Cronin, and M. S. Dresselhaus, Phys. Rev. B **63**, 085406 (2001).
[6] Corning, Inc., Danville, VA, USA, Vycor-7930 glass.
[7] J. Heremans, C. M. Thrush, Y.-M. Lin, S. Cronin, Z. Zhang, M. S. Dresselhaus, and J. F. Mansfield, Phys. Rev. B **61**, 2921 (2000).
[8] R. R. Heikes and R. W. Ure, *Thermoelectricity: Science and Engineering* (Interscience Publishers, New York, 1961), p. 315.
[9] A. G. Hoyem, Phys. Rev. **38**, 1357 (1931).
[10] D. E. Beutler and N. Giordano, Phys. Rev. B **38**, 8 (1988).